ISSN: 0976-3031

Available Online at http://www.recentscientific.com

International Journal of Recent Scientific Research
Vol. 7, Issue, 11, pp. 14466-14473, November, 2016

International Journal of Recent Scientific Research

Research Article

UTILIZATION OF FLY ASH: SYNTHESIS, SPECTRAL, THERMAL STUDIES OF PANI-FA MATRIX COMPOSITES

Clara Jeyageetha J.*, Sankaragomathi V., Bharathi M., Muthumari R and Siji Priya P

Department of Chemistry, A.P.C Mahalaxmi College for Women,
Thoothukudi-628002, India

ARTICLE INFO

Article History:

Received 17th August, 2016
Received in revised form 21th September, 2016
Accepted 28th October, 2016
Published online 28th November, 2016

Key Words:

Polyanilne, Fly ash, FTIR, UV-Vis, SEM-EDXS, TGA

ABSTRACT

Among the electrically conducting polymers, polyaniline (PANI) has attracted more interest due to its advantages over the others, such as easy synthesis, low cost, good processability, high environment stability, and reversible control of electrical properties by both charge-transfer doping and protonation. In India, about 75% of the electricity is generated by coal-based thermal power plants that produce 6.5×10^7 tons per year of fly ash as a by-product. In this chapter, we tried to convert fly ash from waste material into resource material by synthesizing PANI-FA composites from chemical oxidation method in various compositions and characterized. The functional group was analyzed by Fourier Transform Infra red spectroscopy (FTIR). The band gap energy was determined by UV-Vis spectroscopy and photoluminescence spectroscopy. The crystallite size was determined by X-Ray Diffractometry (XRD). The surface morphology was studied by Scanning Electron Microscopy (SEM) and Transmission Electron Microscopy. SEM images revealed that the PANI-FA 45% composite incorporation of fly ash spherical balls in PANI particles which are homogeneously distributed throughout the composites. The elemental composition of the composites was found out by Energy dispersive X-ray spectroscopy (EDXS). Thermal behavior of composites was analyzed by Thermo gravimetric analysis (TGA). The TGA results showed that the presence of FA in the composites could improve the thermal stability up to 180°C. The PL emission spectrum intensity increased with the addition of fly ash to PANI.

INTRODUCTION

With the rise in environmental pollution and the rapid growth of portable electronics, high-efficiency energy storage devices such as super capacitors have become the most promising vehicles in the last decades. Super capacitors, also called electrochemical capacitors, are a kind of high-performance energy storage devices possessing a long life cycle and high power density (Zhang and Zhao, 2012). The synthesis of novel conducting polymers and study of their physical properties has been of prime importance. Aqueous electrochemical process in an environmentally friendly and efficient technique used to process conducting polymer. It is widely preferred because of its simplicity and it can be used as a one step method to form polymer. It allows efficient control of the physiochemical properties of the coatings and it can be easily scaled up for large-scale production (Chiang and Mac Diarmid, 1986).

Conductive polymers had been the topic of the large number of investigations during last decades because of their unique properties such as mechanical strength, electrical conductivity, corrosion, stability and possibility of both oxidative and electrochemical synthesis. Hence PANI is useful in wide area of application: such as solar energy conversion, rechargeable batteries, electro chromic displays, electrochemical sensors, capacitors and active corrosion protector (Tallman *et al*., 2002). Due to ease of synthesis, processing environmental stability and low synthetic cost, so polyaniline is probably the most important industrial conducting polymer today (Wessling and Posdorfer, 1999; Hermelin *et al*., 2001). PANI can be synthesized electrochemically or chemically by using an appropriate oxidant in an acidic medium. There are three forms of PANI, fully oxidized pernigraniline, half-oxidized emaraldine base (EB), and fully reduced leucoemaraldine base (LB) (Norden and Krumeirjer, 2000; Pud *et al*., 2003; Albuquerque *et al.,* 2000). Emaraldine is said to be the most stable form of PANI and it is the most conductive form when it is doped (emaraldine salt).

Fly ash is generally captured from the chimneys of coal-fired power plants, whereas bottom ash is removed from the bottom of the furnace. In the past, fly ash was generally released into the atmosphere, but pollution control equipment mandated in recent decades now requires that it be captured prior to release.

Corresponding author:* **Clara Jeyageetha J
Department of Chemistry, A.P.C Mahalaxmi College for Women, Thoothukudi-628002, India

Depending upon the source and makeup of the coal being burned, the components of the fly ash produced vary considerably, but all fly ash includes substantial amounts of silicon dioxide (SiO_2) (both amorphous and crystalline) alumina (Al_2O_3), iron oxide (Fe_2O_3) and titanium oxide (TiO_2) and calcium oxide (CaO). The disposal of the fly ash is a serious hazard to the environment that consumes millions of rupees towards the cost of its disposal. The mineralogical, physical and chemical properties of fly ash (Shafig *et al*., 2007; Somerset and Vernon, 2003) depend on the parent coal, conditions of combustion, type of emission control devices and storage and handling methods. Therefore, ash produced by burning of anthracite, bituminous and lignite coal has different compositions.

The preference to use fly ash as a filler or reinforcement in metal and polymer matrices is that fly ash is a byproduct of coal combustion, available in very large quantities at very low costs since much of this is currently land filled. Currently, the use of manufactured glass micro spheres has limited applications due mainly to their high cost of production. Therefore, the material costs of composites can be reduced significantly by incorporating fly ash into the matrices of polymers and metallic alloys. The high electrical resistivity, low thermal conductivity, and low density of fly ash may be helpful for making lightweight insulating composites. It also improves the maintainability, damping capacity, coefficient of friction etc. that are needed in various industries like automotive etc.

The present study was carried out to synthesize PANI-FA composites with various weight percentage of fly ash by chemical oxidization method and characterization using FTIR, UV-Vis, XRD, SEM-EDXS, TEM, TGA and PL to find the utilization of this polymer-FA composites and to avoid fly ash as a pollutant into environment and make into resource material.

Experimental Methods

Aniline, Potassium persulphate, HCl, was all the products from Ranbaxy Chemicals. Fly ash (FA) sample was collected from Electrostatic precipitator of Tuticorin Thermal Power Station. All chemicals were used as such and aniline was distilled prior to use.

Synthesis of Polyaniline-Fly ash composites

The method used to prepare PANI-FA was chemical oxidization method [4]. 0.1 M aniline was prepared in 2 M HCl solution. 100 mL of this aniline solution was stirred and FA was added in the solution with vigorous stirring (0%, 15%, 25%, 35%, 45 and 55% FA to aniline w/w ratio). The mixture was kept in an ice bath with continuous stirring. Then 0.1 mol of ammonium persulphate (APS) was added slowly to the aniline solution until the reaction mixture turned green. The reaction mixture was then stirred for 8 h. The product was collected by filtration and washed with water and acetone until the washing was colorless. The collected samples were dried at room temperature and preserved for further studies.

Analytical Methodsp

FTIR spectra were recorded as KBr pellet on a Nicolet iS5 FTIR spectrophotometer in the frequency range 400-4000 cm^{-1} with a resolution of 0.1 cm^{-1} for the determination of functional group. Computer controlled JASCO V-530 was used to study UV-VIS spectral behavior. X-ray diffraction (XRD) was carried on Philips PW1710 automatic X-ray diffractometer with Cu-Kα radiation (λ=1.5404Å), with a scanning speed of 10° min^{1}. The surface morphology was studied with the help of Scanning Electron Microscope (JEOL Model JSM - 6390LV). Elemental composition was determined by Energy Dispersive X-ray Spectroscopy (EDXS). The particle size was characterized by computer controlled PHILIPS CM200 operating voltages: 20-200kv Resolution: 2.4A^0 Transmission Electron Microscopy (TEM). Thermo gravimetric analysis (TGA) of the synthesized polyaniline –fly ash 45 % composite was performed using a TGA-51 Shimadzu in the temperature range of 150.00°C to 955.00°C at 10.00°C/min under N_2 and air atmosphere (flow rate: 50 mL min^{-1}), respectively. A crucible of platinum containing 7 mg of sample was used in the TGA analysis. The PL spectra were taken using Perkin Elmer LS 45 fluorescence spectrometer.

RESULTS AND DISCUSSION

The synthesized PANI-FA composites were characterized by different techniques**.**

Fourier Transform Infrared Spectroscopy (FTIR)

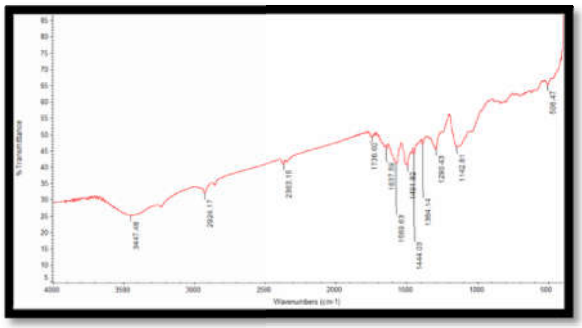

Fig.1 FTIR spectrum for PANI

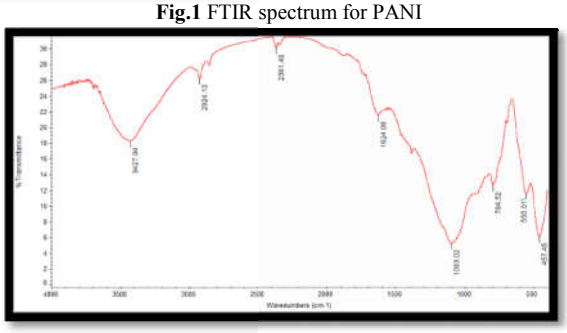

Fig.2 FTIR spectrum for Fly ash

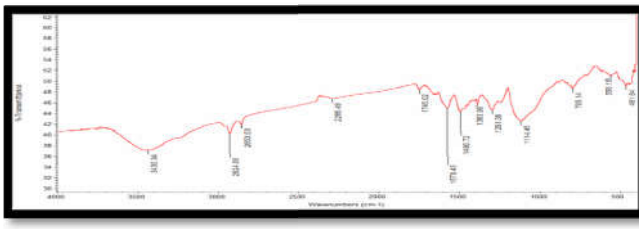

Fig.3 FTIR spectrum for PANI-FA 45 %

FTIR spectra of PANI, FA and PANI-FA % composites are shown in **Fig 1- 3**. FTIR band at 3430-3448 cm^{-1} responds to the N-H stretching with hydrogen bonded amino groups. The absorption band 2924 cm^{1} are assigned to the aromatic sp^2 hybridized C-H stretching vibration mode and aliphatic hydrocarbon C-H stretching due to $-CH_2-$ bonded with aniline unit. The absorption bands observed at 1569 and 1491 cm^{1} in PANI is assigned respectively to the non-symmetric vibration mode of C=C in quinoid and benzenoid ring system in polyaniline. The C-N stretching vibration mode in aromatic amine nitrogen (quinoid system) in doped polyaniline is found at 1290 cm^{1}, corresponding to the oxidation or protonation state. N plane vibration of C-H bending mode in N = Q = N, Q-N^{+}H-B or B-N^{+}H-B (where Q = quinoid and B = benzenoid) is observed at 1142 cm^{1}. The presence of this absorption band is expected due to the polymerization of PANI, *i.e.*, polar structure of the conducting protonated form (Rees *et al*., 2007). In FTIR spectrum of purified FA, the characteristic 3427 cm^{1} band indicating the stretching vibration of the -OH group appears due to some components with an -OH group or crystal lattice water on the surface of FA. The IR spectrum of the PANI-FA composite in most of the cases resembles that of PANI indicating the existence of PANI in the emeraldine salt form. The broadening of the peak could be due to the merging of the IR peaks that arise from the absorption of the various metal oxides present in FA (Raghavendra *et al*., 2003).

UV-Visible Spectroscopy

The absorption spectra of PANI-FA composites, Polyaniline and Fly ash are shown (Fig 4-6). In our present study the pure PANI exhibited an absorption peak at 354 nm owing to the π-π* transition of the benzenoid ring. The band located at 600 nm corresponds to the benzenoid-to-quinoid ring. On the other hand, the absorption peak of PANI-FA 45 % composite visible at 378 nm display red shift of 24 nm as compared to that of PANI. It may be due to the improved intermolecular interaction and very high band gap of the composites. The peaks with maximum wavelength at 370-400 nm for the PANI-FA composites may be due to a conjugated benzenoid band associated with π-π* transition. This confirmed the presence of benzene ring in polyaniline. The peaks at 550-600 nm is due to n- π* transitions of quinoid ring (Vivekanandan *et al*., 2011; Stejskal *et al*., 2004).

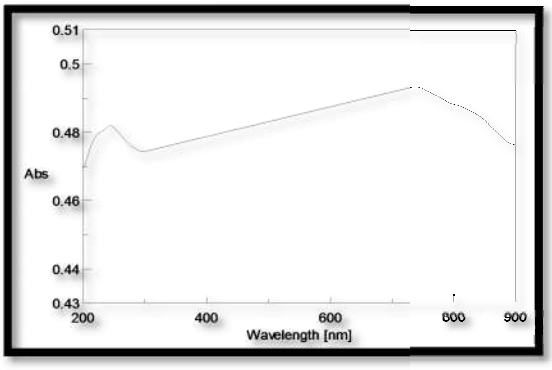

Fig.4 UV-Vis Spectrum of fly ash

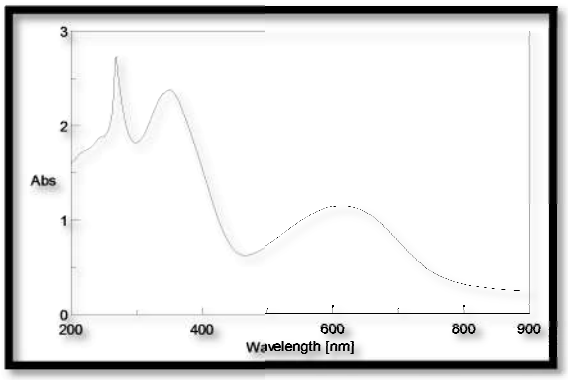

Fig. 5 UV-Vis Spectrum of PANI

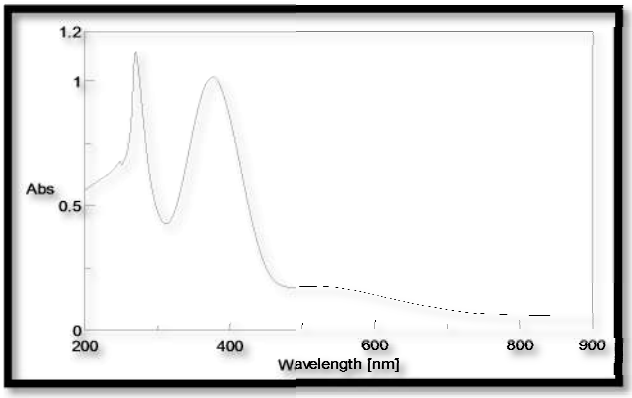

Fig.6 UV-Vis Spectrum of PANI-FA45%

In this present study (Fig 4) shows UV-Vis absorption spectra of fly ash. Fig 5 & Fig 6 shows the band at 370-400 nm may be due to a conjugated benzenoid band associated with π-π* transition. (Vivekanandan *et al*., 2011; Stejskal *et al*., 2004). The characteristic bands due to π-π* transition at 375 nm and the band due to the inter-ring charge transfer associated with excitation from benzenoid to quinoid moieties at 550 nm (Rao *et al*., 2012; Jessica and Chinnapayan, 2015). PANI–FA composite showed clear similarity in their UV-Vis spectra particularly with the presence of the absorption maxima at 370-400 nm and 550-600 nm which is associated with the stabilization of the composite in the emeraldine form. There was a close agreement with the results of UV-Vis and FTIR.

Band Gap Energy

The calculation of band gap energy (Table 1) is a convenient way of studying the optical absorption of material.

Table 1 Band gap Energy for Fly ash, PANI and composites

Samples	Band gap energy (eV)
Fly ash	5.13 (λ_{max} = 240 nm) &1.65 (λ_{max} =746nm)
PANI	4.52 (λ_{max} = 272 nm) 3.47 (λ_{max} = 354 nm) & 2.05 (λ_{max} =600 nm)
PANI-FA 45%	4.63 (λ_{max}= 266 nm), 3.25 (λ_{max}= 378 nm) & 2.22 (λ_{max} =554 nm)

X-Ray Diffraction Studies (XRD)

XRD was studied for the prepared PANI-FA 45% composite is shown in Fig 7.

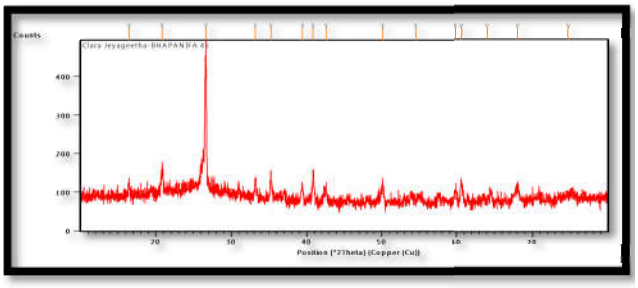

Fig.7 X-ray Diffraction spectrum of PANI-FA 45% composite

XRD pattern of PANI-FA 45 % showed the characteristics peaks at 2θ = 20.8° and 26.6°, corresponding to the (100) and (101) reflection planes of quartz of fly ash. The peaks at 35.2° (104), shows the presence of crystalline Al_2O_3 of FA. Pure PANI **(JCPDS card No. 53-1891)** showed a characteristic XRD peak at 2θ = 25.9°, that corresponds to the emeraldine salt (ES-I) phase of the polymer. As reported earlier by Raghavendra *et al.,* (2003), the PANI-FA composites showed a sharp peak at 2θ = 26.6°, which is evident in our XRD results (Fig 7). As the FA concentration increased, the height of 2θ = 25.9° PANI peak gradually diminished and a peak around 2θ = 26.6°, increased and became more prominent. This new peak was essentially a combination of the PANI peak (2θ = 25.9°) and the peaks due to the constituents of FA around the same 2θ value. Therefore, as the FA concentration increases, the PANI peak gradually disappears. In the XRD plots, this occurs as a gradual shift of peaks near 2θ = 25.9° towards slightly higher 2θ values.

SEM-EDXS

A Scanning Electron Microscope (SEM) (model-JEOL-JSM-6380LA) with energy dispersive X-ray Spectroscopy (EDXS) was used to evaluate the texture, morphology and elemental composition of PANI-FA 45 % composite.

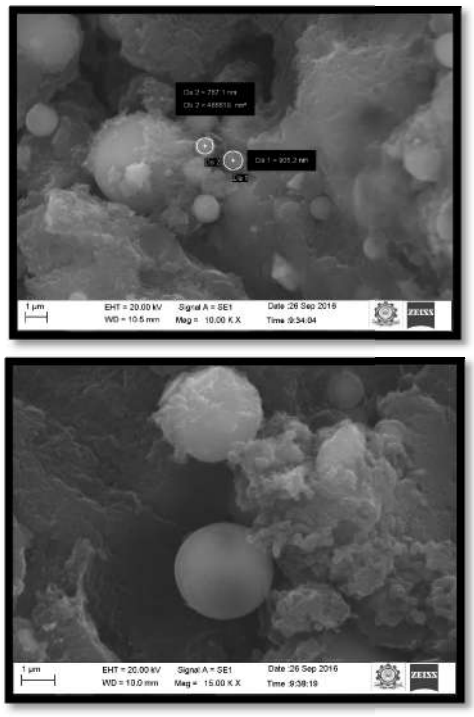

Fig.8-9 SEM images of PANI-FA 45 %

In our present study, the SEM image (Fig 8-9) of PANI-FA 45% composite clearly showed the incorporation of fly ash spherical balls in PANI particles which are homogeneously distributed throughout the composites, which is also confirmed from XRD studies. These cenospheres showed a large variation in their dimensions. The cenosperes with diameter of 787.1 nm and 905.2 nm was recorded. The variation in the dimensions of cenospheres depends on the conditions of the thermal plants during which the FA has been expelled out. Such a large variation in the dimensions of cenospheres has a strong influence on the various electrical properties of the composites. Since the particles of FA are spherical in shape, the observed porosity in these composites is less than the other PANI composites (Chowdhury *et al.,* 2002).

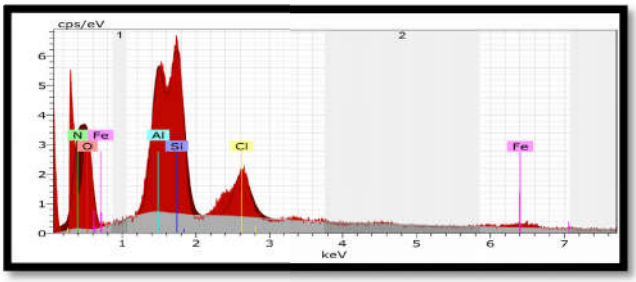

Fig.10 EDXS for PANI-FA 45 %

Table 2 Elemental composition of PANI-FA 45 %

Element	Unn.C [wt.%]	Norm.C [wt.%]	Atom.C [at.%]	Error (3sigma) [wt.%]
Oxygen	27.33	41.51	44.50	10.66
Nitrogen	21.91	33.29	40.76	8.72
Silicon	6.59	10.02	6.12	0.93
Aluminium	6.54	9.94	6.32	1.02
Iron	0.86	1.30	0.40	0.17
Chlorine	2.60	3.94	1.91	0.35
Total	65.83	100.00	100.00	

The composite of PANI-FA 45 % showed (Fig 10) major elements of oxygen, nitrogen, silicon and aluminium. Minor elements were found iron and chlorine. Nitrogen due to the presence of aniline in the composite and silicon and aluminium confirmed the presence of Fly ash in the composite. The elemental composition of PANI-FA 45% composite is shown in the Table 2. The fly ash chemical composition usually depends on their sources. In this study, the elemental composition of the composite 45% was verified using EDXS.

Transmission Electron Microscope (TEM)

In our present study TEM images of PANI-FA 45 % (Fig 11-12) at three different resolutions nanosize turmeric shape structure with uniform interconnected distribution was studied. The particles were irregularly shaped and aggregated. There was a clear indication from the image that fly ash is entrapped with PANI matrix as a result there is an integrated morphology.

It was found that FA has a strong effect on the PANI's morphology; it shows a transformation in morphology of PANI particles. It can also be seen that the spherically shaped FA particles are uniformly dispersed in the PANI matrix. The Selection Area Electron Diffraction (SAED) pattern showed the particle size to be 100nm.

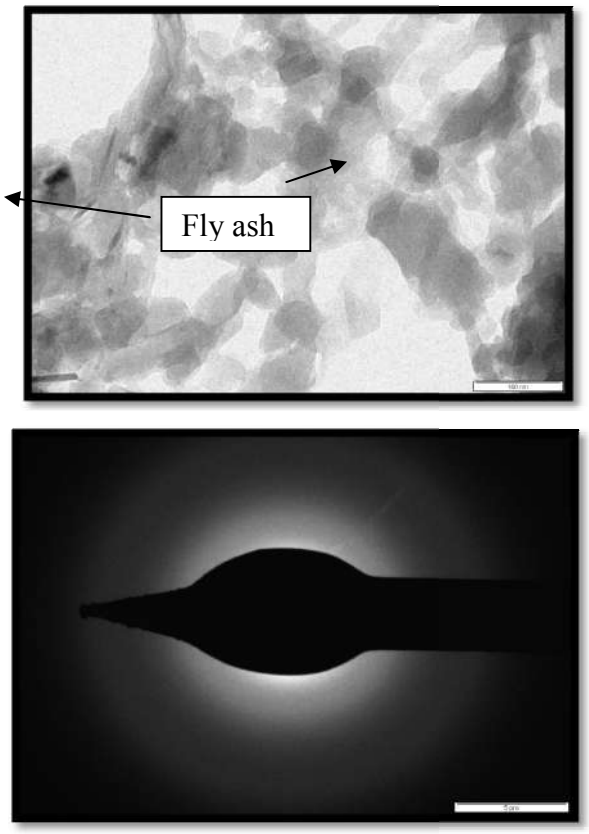

Fig.11-12 TEM images of PANI-FA 45%

Thermo gravimetric analysis (TGA)

TGA is widely used to study all physical process involving the weight changes such as to measure the diffusion characteristics and the moisture uptake of a sample.

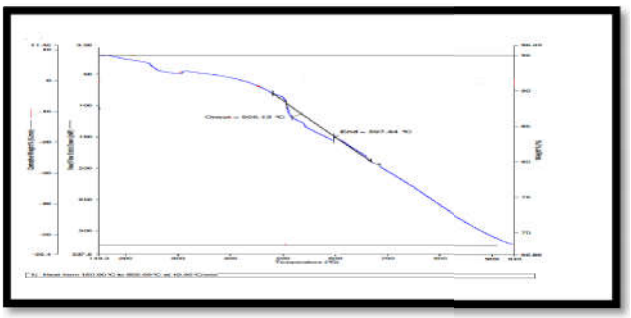

Fig.13 Thermo gram of PANI-FA 45 %

The thermo gravimetric profile of PANI-FA 45 % polymer composite is shown in Fig 13**.** The thermo gram weight loss indicated the interaction of PANI with the metal oxides such as Al_2O_3 and SiO_2 present in FA. FTIR spectra also confirmed the interaction of SiO_2 and PANI. This may be due to the Vander Waals binding of PANI-FA polymer composites. The thermo gram of PANI-FA 45 % composite showed three major steps of weight loss. In the first step, the initial weight loss at 1-2 % up to 180^{o}C may be due to the removal of moisture present in the polymer (Rees *et al*., 2007).

In the second step 2-3 % weight loss continued from 180- 320^o C suggested that the evolution of thermally labile compounds, the breaking of aliphatic structures with low dissociation bonds in the carbonaceous matrix of FA and the removal of acid dopant. There is a moderate weight loss from 490^{o}C may be associated with the degradation of the polyaniline backbone of the composites. The onset temperature of the degradation of PANI was observed to be around 506^o C accompanied by massive weight loss towards higher temperature. In the third step the weight loss of 5-6 % in the range of 490- 680^o C indicated that the release of shoot particles attached with SiO_2 system of FA and degradation of the skeletal polyaniline chain structure (Malhotra *et al*., 2006, Kaushik *et al*., 2009). Above 700^o C strong weight loss was observed due to thermal degradation of mineral matter of fly ash.

Photoluminescence Spectroscopy (PL)

PL spectra were measured for the three samples of polyaniline, fly ash, PANI-FA 45% composite in the range of 200-900 nm and shown in Fig 14-16. The wavelength of excitation chosen for all the samples is 320 nm. This is because π-π* transition of the benzenoid unit is responsible for PL in PANI (Veluru *et al*., 2013). PANI-FA 45% composite showed a better PL intensity, the possible reason may be that benzenoid and quinoid units are more orderly arranged in it which favors the formation of excitons and increase in delocalization length of a singlet exciton (Shimano and Mac Diarmid, 2001; Wohlgenannt and Vardney, 2003).

Morphological study for system-4 was done with TEM analysis shown in Fig. 7, which confirms the formation of homogeneous interconnected composite system. TEM images of system-4 (PANI/MWCNTs/ Starch) at three different resolutions 500nm, 200 nm, and 100 nm. We observed nanosize turmeric shape structure (nanorod size ┐ 200 nm in length and < 50 nm in width) with uniform interconnected distribution. From micro-graph at 500 nm resolution it is clearly visible that the material has porous network like architecture. Such finger like structure suggested that PANI and Starch coated over the surface of MWCNTs (which act as a template for the deposition. There is clear indication from the images that MWCNTs and Starch are entrapped within PANI matrix as a result there is an integrated morphology. There are dwelling spaces and such morphology is suitable for the immobilization of biomolecule Morphological study for system-4 was done with TEM analysis shown in Fig. 7, which confirms the formation of homogeneous interconnected composite system. TEM images of system-4 (PANI/MWCNTs/ Starch) at three different resolutions 500nm, 200 nm, and 100 nm. We observed nanosize turmeric shape structure (nanorod size ┐ 200 nm in length and 50 nm in width) with uniform interconnected distribution. From micro-graph at 500 nm resolution it is clearly visible that the material has porous network like architecture. Such finger like structure suggested that PANI and Starch coated over the surface of MWCNTs (which act as a template for the deposition. There is clear indication from the images that MWCNTs and Starch are entrapped within PANI matrix as a result there is an integrated morphology. There are dwelling spaces and such morphology is suitable for the immobilization of biomolecu Morphological study for system-4 was done with TEM analysis shown in Fig. 7, which confirms the formation of homogeneous interconnected composite system. TEM images of system-4 (PANI/MWCNTs/ Starch) at three different resolutions 500nm, 200 nm, and 100 nm. We observed nanosize turmeric shape structure (nanorod size □ 200 nm in length and < 50 nm in width) with uniform interconnected distribution. From micro-

graph at 500 nm resolution it is clearly visible that the material has porous network like architecture. Such finger like structure suggested that PANI and Starch coated over the surface of MWCNTs (which act as a template for the deposition. There is clear indication from the images that MWCNTs and Starch are entrapped within PANI matrix as a result there is an integrated morphology. There are dwelling spaces and such morphology is suitable for the immobilization of biomolecule Morphological study for system-4 was done with TEM analysis shown in Fig. 7, which confirms the formation of homogeneous interconnected composite system. TEM images of system-4 (PANI/MWCNTs/ Starch) at three different resolutions 500nm, 200 nm, and 100 nm. We observed nanosize turmeric shape structure (nanorod size ┐ 200 nm in length and < 50 nm in width) with uniform interconnected distribution. From micro-graph at 500 nm resolution it is clearly visible that the material has porous network like architecture. Such finger like structure suggested that PANI and Starch coated over the surface of MWCNTs (which act as a template for the deposition. There is clear indication from the images that MWCNTs and Starch are entrapped within PANI matrix as a result there is an integrated morphology. There are dwelling spaces and such morphology is suitable for the immobilization of biomolecule Morphological study for system-4 was done with TEM analysis shown in Fig. 7, which confirms the formation of homogeneous interconnected composite system. TEM images of system-4 (PANI/MWCNTs/ Starch) at three different resolutions 500nm, 200 nm, and 100 nm. We observed nanosize turmeric shape structure (nanorod size ┐ 200 nm in length and < 50 nm in width) with uniform interconnected distribution. From micro-graph at 500 nm resolution it is clearly visible that the material has porous network like architecture. Such finger like structure suggested that PANI and Starch coated over the surface of MWCNTs (which act as a template for the deposition. There is clear indication from the images that MWCNTs and Starch are entrapped within PANI matrix as a result there is an integrated morphology. There are dwelling spaces and such morphology is suitable for the immobilization of biomolecu Morphological study for system-4 was done with TEM analysis shown in Fig. 7, which confirms the formation of homogeneous interconnected composite system. TEM images of system-4 (PANI/MWCNTs/ Starch) at three different resolutions 500nm, 200 nm, and 100 nm. We observed nanosize turmeric shape structure (nanorod size ┐ 200 nm in length and < 50 nm in width) with uniform interconnected distribution. From micro-graph at 500 nm resolution it is clearly visible that the material has porous network like architecture. Such finger like structure suggested that PANI and Starch coated over the surface of MWCNTs (which act as a template for the deposition. There is clear indication from the images that MWCNTs and Starch are entrapped within PANI matrix as a result there is an integrated morphology. There are dwelling spaces and such morphology is suitable for the immobilization of biomolecule orphological study for system-4 was done with TEM analysis shown in Fig. 7, which confirms the formation of homogeneous interconnected composite system. TEM images of system-4 (PANI/MWCNTs/ Starch) at three different resolutions 500nm, 200 nm, and 100 nm.

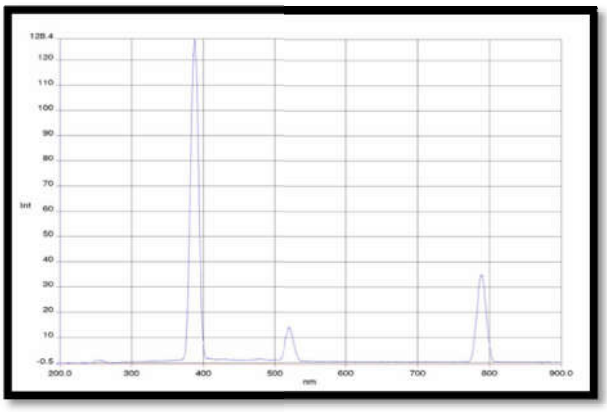

Fig.14 Photoluminescence spectrum of PANI

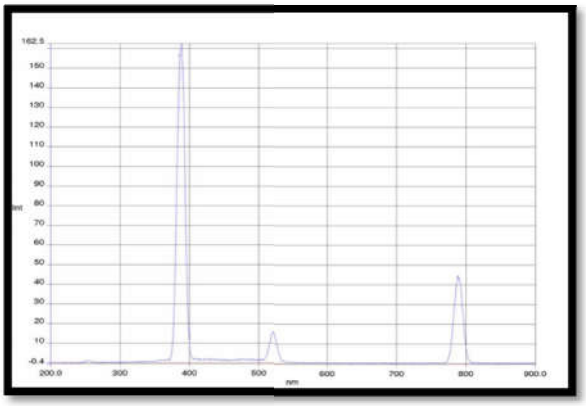

Fig.15 Photoluminescence spectrum of Fly ash

We observed nanosize turmeric shape structure (nanorod size ┐ 200 nm in length and < 50 nm in width) with uniform interconnected distribution. From micro- graph at 500 nm resolution it is clearly visible that the material has porous network like architecture. Such finger like structure suggested that PANI and Starch coated over the surface of MWCNTs (which act as a template for the deposition. There is clear indication from the images that MWCNTs and Starch are entrapped within PANI matrix as a result there is an integrated morphology. There are dwelling spaces and such morphology is suitable for the immobilization of biomolecule

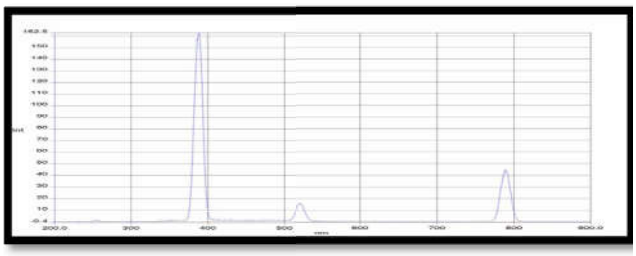

Fig.16 Photoluminescence spectrum of PANI-FA 45%

In our present study PANI showed peak with low intensity compared fly ash and PANI-FA 45 % composite. The species responsible for PL emission in PANI is the benzenoid unit (Sainz *et al.,* 2005; Shimano and MacDiarmid, 2001). PANI-FA 45% composite showed greater intensity than PANI. The intensity of the emission peak of all the three samples centered on 260 and 525 nm are much smaller. In the spectrum of composite, it was seen that the PL emission spectrum intensity increased with the addition of fly ash to PANI. Around 390 nm region the samples was showing intense and sharp PL emission

peak. The enhancement of the PL emission intensity in the composite can be explained there are electro donating groups such as >NH in PANI and electron with drawing groups in fly ash. This combination enhances the electron mobility in the composite.

Band gap energy determination by PL spectrum for PANI-FA composite and compared with UV-Vis spectrum

The absorption peak at 4.63 eV found in UV-Vis (Table 2) has been confirmed. This is in close agreement with 4.73 eV PL peak. The absorption peak at 3.25 eV in UV-Vis confirmed the close agreement with 3.15 eV of PL peak corresponding to π-π* transition of the benzenoid ring. The third peak at 2.22 eV in UV-Vis was confirmed by close agreement with 2.34 eV of PL peak corresponding to π-π* transition of the quinoid ring of PANI which indicated the doped PANI.

CONCLUSION

In this study, we made a successful conversion of fly ash from waste material into resource material by the incorporation of PANI matrix. PANI-FA composites were synthesized by chemical oxidation method. From TEM images, there was a clear indication of fly ash are entrapped with PANI matrix as a result there is an integrated morphology. It was found that FA has a strong effect on the PANI's morphology; it shows a transformation in morphology of PANI particles. It can also be seen that the spherically shaped FA particles were uniformly dispersed in the PANI matrix. The TGA results revealed that the fly ash improved the stability of PANI. These composites may become promising for advanced materials to be used in the high-technology industries in the future. In addition, these materials can reduce the cost due to usage of FA.

Acknowledgements

The authors wish to thank Dr.Chinnapiyan Vedhi, Assistant Professor, PG and Research Department of Chemistry, V.O Chidambaram College, Tuticorin, Tamil Nadu, India for supporting this successful project work.

References

1. Albuquerque, J.E., Mattoso, L.H.C., Balogh, D.T., Faria, R.M., Masters, J.G. and MacDiarmid, A.G. (2000): A Simple Method to Estimate the Oxidation State of Polyanilines, Synth. Met., 113:19-22.
2. Chiang, J.C. and Mac Diarmid, A.G. (1986): 'Polyaniline': Protonic acid doping of the emeraldine form to the metallic regime. Synthetic Metals., 13(1–3): 193-205.
3. Chowdhury, A. N., Yousuf, M. A, Rahman, M .M. and Hassan, A. Q .M .Q. (2002): *Indian J. Chem*., A41: 1562.
4. Hermelin, E., Petitjean, J., Aeiyach, S., Lacroix, J.C. and Lacaze, P.C. (2001): Industrial polypyrrole electro deposition on zinc electroplated steel. *J. Appl. Electrochem*., 31: 905.
5. Jessica F. and Chinnapiyan V, (2015): Synthesis, Spectral and Electrochemical Characterization of Adipic Acid Doped Polyaniline. *The International Journal of Science & Technoledge*., 3(4).
6. Kaushik, A., Khan, R., Gupta, V., Malhotra, B.D. and Singh, S.P. (2009): Hybrid Cross-Linked Polyaniline - WO3 Nano- Composite Thin Film Using Thermal Vacuum Deposition Technique for NOx Gas Sensing. *Journal of Nanoscience & Nanotechnology*., .9: 1792-1796.
7. Malhotra, B.D., Chaubey, A. and Singh, S.P. (2006): Prospects of Conducting Polymers in Biosensors. Analytica Chimica Acta., 578: 59-74.
8. Norden, B. and Krumeirjer, E. Noble prize in chemistry, (2000): Conducting polymers; the royal Swedish Academy of science; [online] www.kva.se
9. Pud, A., Orgurtsov, N., Korzhenko, A. and Shapoval, G. (2003): Some aspects of preparation and properties of Polyaniline blends and composites with organic polymers; Progress in Polymer Science, (28), pp. 1701-1753.
10. Raghavendra, S.C., Syed khasim, Revanasiddapp, M., Ambika Prasad, M.V.N. and Kulkarni, A.B. (2003): Synthesis, characterization and low frequency a.c. conduction of polyaniline/fly ash composites. Bull. Mater. Sci., 26(7): 733–739.
11. Rao, C.R.K., Muthukannan, R. and Vijayan, M. (2012): Studies on biphenyl disulphonic acid doped polyanilines: Synthesis, characterization and electrochemistry. Bull Mater Sci., 35:405
12. Rees, C.A., Provis, J.L., Lukeya, G.C. and Van Deventer, J.S.J. (2007): Attenuated Total Reflectance Fourier Transform Infrared Analysis of Fly Ash Geopolymer Gel Aging, Langmuir. 23:8170-8179.
13. Sainz, R., A., Benito, M., Martinez, M.T., Galindo, J.F., Sotres, J., Baro, A.M., Corraze, B., Chauvet, O., Dalton, A.B., and Baughman, R.H. and Maser,W.K. (2005): Nanotechnol.,16:S 150.
14. Sathiyanarayanan, S., Azim, S.S. and Venkatachari, G. (2007) Preparation of Polyaniline–Fe_2O_3 Composite and Its Anticorrosion Performance. Synth.Met., 157:751-757.
15. Shafiq, N., Nuruddin, M.F. and Kamaruddin, I. (2006): In: Cement and Concrete Science Conference No. 26, Sheffield Hallam University, UK. Adv. Appl.Ceram., 2007. 106 (6): 314-318.
16. Shimano, J.Y. and MacDiarmid, A.G. (2001): Polyaniline, a Dynamic Block Copolymer: Key to Attaining Its Intrinsic Conductivity?. Synthetic Metals., 123(2):251-262.
17. Somerset, and Vernon Sydwill, 2003. The preparation and characterization of high capacity ion exchange adsorbents made by co-disposal of fly ash and acid mine drainage, and their use in electrochemical systems for water purification. Master's Thesis, Department of Chemistry, University of Western Cape, South Africa.
18. Stejskal , J., Hlavata , D., Holler, P., Trchova , M., Prokes , J. and Sapurina, I. (2004): Poly Int, 53: 294.
19. Tallman, D.E., Spinks, G., Dominis, A. and Wallace, G.G. (2002): Electroactive conducting polymers for corrosion. J.Solid state Electrochem., 6: 85.
20. Veluru Jagadeesh Babu, Sesha Vempati, and Seeram Ramakrishna, (2013): Conducting Polyaniline-Electrical Charge Transportation, Materials Sciences and Applications.
21. Vivekanandan, J., Ponnusamy, V., Mahudeswaran, A. and Vijayanand, P.S. (2011): Synthesis, characterization

and conductivity study of polyaniline prepared by chemical oxidative and electrochemical methods Scholars research library Archives of Applied Science Research., 3 (6):147-153.

22. Wessling, B., and Posdorfer, J., (1999): Polyaniline/epoxy coatings with good anti-corrosion properties. Synthetic Metals., 102: 1400-1401.
23. Wohlgenannt, M. and Vardeny Z.V. (2003): Spin-dependent Exciton Formation Rates in π-Conjugated Materials. *Journal of Physics: Condensed Matter*, 15(3).
24. Zhang, J. and Zhao, X. (2012): On the configuration of super capacitors for maximizing electrochemical performance. Chem. Sus. Chem., 5: 818–841.

****

How to cite this article:

Clara Jeyageetha J. *et al*, 2016, Utilization of fly ash: Synthesis, Spectral, Thermal Studies of Pani-fa Matrix Composites. *Int J Recent Sci Res.* 7(11), pp. 14466-14473.